

Aspects for calculating local absorption with the rigorous coupled-wave method

Karl-Heinz Brenner*

Chair of Optoelectronics, University of Heidelberg, B6, 23-29 68131 Mannheim, Germany
*brenner@ziti.uni-heidelberg.de

Abstract: The calculation of local absorption is very important in the context of lithography and in photo-detector design. We present a rigorous method for calculating the local absorption in periodic structures. The computation depends primarily on the calculation of the electric field inside the structure. Since the standard definitions produce unsatisfactory results, we use a modified version of a method published by Lalanne [J. Modern Opt. **45**, 1357 (1998)]. The results for these field definitions agree very accurately with results obtained by the law of conservation of energy. We present some examples which are typical for the application scenarios of lithography and detectors.

©2010 Optical Society of America

OCIS codes: (050.1755) Computational electromagnetic methods, (050.1960) Diffraction theory, (260.2110) Electromagnetic optics, (260.2160) Energy transfer

References and links

1. N. Moll, T. Morf, M. Fertig, T. Stoferle, B. Trauter, R. F. Mahrt, J. Weiss, T. Pfluger, and K.-H. Brenner, "Polarization-Independent Photodetectors With Enhanced Responsivity in a Standard Silicon-on-Insulator Complementary Metal–Oxide–Semiconductor Process," J. Lightwave Technol. **27**(21), 4892–4896 (2009).
 2. M. G. Moharam, E. B. Grann, D. A. Pommet, and T. K. Gaylord, "Formulation for stable and efficient implementation of the rigorous coupled-wave analysis of binary gratings," J. Opt. Soc. Am. A **12**(5), 1068–1076 (1995).
 3. Ph. Lalanne, and G. M. Morris, "Highly improved convergence of the coupled-wave method for TM polarization," J. Opt. Soc. Am. A **13**(4), 779–784 (1996).
 4. P. Lalanne, and E. Silberstein, "Fourier-modal methods applied to waveguide computational problems," Opt. Lett. **25**(15), 1092–1094 (2000).
 5. P. Lalanne, and M. P. Jurek, "Computation of the near field pattern with coupled wave method for transverse magnetic polarisation," J. Mod. Opt. **45**(7), 1357–1374 (1998).
 6. L. Li, "Use of Fourier series in the analysis of discontinuous periodic structures," J. Opt. Soc. Am. A **13**(9), 1870–1876 (1996).
 7. E. Popov, and M. Neviere, "Maxwell equations in Fourier space: fast converging formulation for diffraction by arbitrary shaped, periodic, anisotropic media," J. Opt. Soc. Am. A **18**(11), 2886–2894 (2001).
 8. T. Schuster, J. Ruoff, N. Kerwien, S. Rafler, and W. Osten, "Normal vector method for convergence improvement using the RCWA for crossed gratings," J. Opt. Soc. Am. A **24**(9), 2880–2890 (2007).
 9. E. Silberstein, P. Lalanne, J.-P. Hugonin, and Q. Cao, "Use of grating theories in integrated optics," J. Opt. Soc. Am. **18**(11), 2865–2875 (2001).
-

1. Introduction

Local absorption is a very useful concept in the context of lithography, where the resist exposure is proportional to the amount of energy which is absorbed in a small volume element. Another important field for local absorption is photo-detector design, where the location of photo-electron generation plays an important role for the responsivity of the photo-diode [1]. Only those electrons, which are generated near the depletion region, contribute to the photo-current, while electrons generated in other regions mostly contribute to local heating. In order to be able to make exact predictions for resist exposure or detector optimization, precise knowledge of the electromagnetic near-field distribution inside a structure is necessary. The rigorous coupled wave analysis (RCWA) [2–5] over the years has developed into a reliable tool for calculating the diffraction efficiencies of dielectric and metallic gratings as well as periodic layers of these materials. Furthermore, the RCWA has also been extended to non-isotropic media [4]. The stability of calculation for step-like

distributions has been improved by Li [6] using rules to satisfy continuity conditions. For discontinuous three-dimensional gratings, normal vector fields have been applied by Popov [7] and recently by Schuster [8] to satisfy more complicated continuity conditions.

Within the RCWA, the global absorption is typically obtained by assuming the law of energy conservation as given and calculating the sum of the reflected and transmitted diffraction orders. The difference to unity is then considered as the global absorption. On the other hand, only little work has been published on calculating the near field distribution inside these structures. Some of the problems associated with near-field calculations have been discussed in [5] and [9]. In the paper, we first observe, that the near field calculation is not uniquely defined. We will first present the concept of local absorption, derived from Poynting's theorem. Then we consider various methods for calculating the electric field distribution from RCWA-data and finally we will discuss some examples.

2. Poynting's theorem and local absorption

The starting point for Poynting's theorem is the Poynting vector for complex electromagnetic fields, which describes the flow of energy per unit of time and area:

$$\mathbf{S} = \frac{1}{2} \text{Re}(\mathbf{E} \times \mathbf{H}^*) \quad (1)$$

Considering the first two Maxwell's equations

$$\begin{aligned} \text{rot } \mathbf{E} &= -\mu\mu_0 \dot{\mathbf{H}} \\ \text{rot } \mathbf{H} &= \mathbf{j} + \varepsilon\varepsilon_0 \dot{\mathbf{E}} \end{aligned} \quad (2)$$

for monochromatic fields, which are proportional to $e^{-i\omega t}$, and taking the divergence of Eq. (1), one obtains the relation:

$$\text{div}(\mathbf{S}) + \frac{\mu\mu_0}{4} \frac{\partial}{\partial t} |\mathbf{H}|^2 + \frac{\varepsilon_r \varepsilon_0}{4} \frac{\partial}{\partial t} |\mathbf{E}|^2 = -\frac{1}{2} \text{Re}(\mathbf{E} \cdot \mathbf{j}^*) - \frac{\text{Im}(\varepsilon) \varepsilon_0}{2} \omega |\mathbf{E}|^2. \quad (3)$$

Here $\varepsilon_0 \mu_0 = c^{-2}$ are the permittivity and permeability of vacuum and μ as well as $\varepsilon_r + i\varepsilon_i$ are the permeability and the complex permittivity of the material. For high frequency optical fields, the current density is usually small and can be ignored. The second and third term of the left hand side express the temporal change of energy density, which is zero for the stationary case. We integrate Eq. (3) over an arbitrary volume. For the first term, we apply the theorem of Gauss and consider the surface normals to be oriented outward:

$$-\oint \mathbf{S}_i \cdot d\mathbf{A} + \oint \mathbf{S}_t \cdot d\mathbf{A} + \oint \mathbf{S}_r \cdot d\mathbf{A} = -\iiint \frac{\text{Im}(\varepsilon) \varepsilon_0}{2} \omega |\mathbf{E}|^2 dV \quad (4)$$

The indices i , t and r correspond to incident, the transmitted and the reflected Poynting vectors. By changing the signs and performing the integration, we can identify the law of power conservation:

$$P_i - P_t - P_r = P_a \quad (5)$$

with

$$P_a = \frac{\varepsilon_0 \omega}{2} \iiint \text{Im}(\varepsilon(\mathbf{r})) |\mathbf{E}(\mathbf{r})|^2 dV \quad (6)$$

which states that the absorbed power in a volume is given by the product of the imaginary part of the epsilon distribution and the magnitude square of the electric field. With real ε dielectrics, the absorbed power is zero. Also, absorption requires a field intensity to be present. With the vacuum impedance $Z_0 = \sqrt{\mu_0 / \varepsilon_0}$ and $\omega = ck_0$, we can conclude, that the power absorbed in a given volume is

$$P_a = \frac{k_0}{2Z_0} \iiint \text{Im}(\varepsilon(\mathbf{r})) |\mathbf{E}(\mathbf{r})|^2 dV \quad (7)$$

For using Eq. (7) in numerical calculations, we split the electric near field as

$$\mathbf{E}(\mathbf{r}) = E_0 \cdot \mathbf{E}_1(\mathbf{r}) \quad (8)$$

with $\mathbf{E}_1(\mathbf{r})$ being the dimensionless response to an incident field with amplitude 1 and E_0 has the dimension of an electric field, i.e. V/m and represents a scaling factor. We can determine E_0 from the power P_i of the incident plane wave with unit direction vector \mathbf{s}_i by

$$P_i = \iint \mathbf{S}_i \cdot d\mathbf{A} = \frac{1}{2Z_0} \sqrt{\frac{\varepsilon_i}{\mu_i}} |E_0|^2 A \cdot s_{i,z} \quad (9)$$

Combining Eq. (7), 8 and 9, we obtain

$$\frac{P_a}{P_i} = \frac{k_0^2}{k_{i,z}} \frac{1}{A} \iiint \text{Im}(\varepsilon(\mathbf{r})) \cdot |\mathbf{E}_1(\mathbf{r})|^2 dV \quad (10)$$

a relation which is independent of Z_0 and E_0 . Here $\mu_i = 1$ was assumed. For the two-dimensional RCWA, i.e. for gratings which vary only in x-direction, the y-direction is constant. By applying a discretisation with $\delta x = Wx / NX$, $\delta z = Wz / NZ$ for the x- and z-direction and expressing the incident area as $A = NX \delta x \delta y$, the factor δy cancels out and the volume integral can be approximated by a Riemann-sum:

$$\frac{P_a}{P_i} = \frac{\delta z}{NX} \frac{k_0^2}{k_{i,z}} \cdot \sum_{j=0}^{NX-1} \sum_{k=0}^{NZ-1} \text{Im}(\varepsilon(x_j, z_k)) \cdot |\mathbf{E}_1(x_j, z_k)|^2 \quad (11)$$

The terms under the sum are now dimensionless quantities which are accessible by the RCWA. Each term under the sum can be identified as the local power absorbed in the volume element j, k . By summation of the local absorption over the whole structure, the Integrated absorption $A_i = P_a / P_i$ is thus obtained and should be equal to the Global absorption obtained from the RCWA as $1 - \sum T_m - \sum R_m$.

3. Absorption and near field calculation in the RCWA

The RCWA primarily serves for calculating the diffraction efficiencies T_m and R_m for each mode m . By applying the law of conservation of energy, the Global absorption of diffractive structures is defined by

$$A_g = 1 - \sum_m (T_m + R_m) \quad (13)$$

3.1 TE-polarisation

For TE-polarisation, the electric field in a layer consists only of the y-component. In the RCWA, the y-component of the electric field is described by

$$E_y(x, z) = \sum_m S_m(z) \exp(ik_{x,m}x) \quad (14)$$

with $k_{x,m} = k_{i,x} + 2\pi \frac{m}{P}$. The vector $\mathbf{S}(z) = \mathbf{W} \cdot \mathbf{C}(z)$ is derived from the eigenvalue problem resulting in the eigenvector matrix \mathbf{W} and the coefficient vector with the components

$C_m(z) = c_m^+ \exp(-k_0 z \sqrt{\lambda_m}) + c_m^- \exp(k_0(z-d) \sqrt{\lambda_m})$. The λ_m are the corresponding Eigenvalues. For perpendicular incidence, i.e. $k_{i,z} = n_i k_0$ the local absorption in a volume element $\delta x \cdot \delta y \cdot \delta z$ can be calculated by

$$a(x_j, z_k) = \frac{k_0}{n_{i,z}} \frac{\delta z}{NX} \text{Im}(\varepsilon(x_j, z_k)) \cdot |E_y(x_j, z_k)|^2 \quad (15)$$

For the calculation of $\text{Im}(\varepsilon)$ there are two possibilities. The most natural would be to take the imaginary part of the spatial distribution of $\varepsilon(x)$. In the examples, we refer to this choice as the original epsilon-distribution (OED). Considering that all the information, the RCWA has about the layer, is a truncated series expansion, one can also calculate ε from the mode expansion

$$\varepsilon(x) = \sum_{m=-M}^M \tilde{\varepsilon}_m \exp\left(2\pi i \frac{mx}{P}\right) \quad (16)$$

where $\tilde{\varepsilon}_m$ is obtained from the standard calculation of Fourier coefficients of a periodic function. We refer to this choice as the “reconstructed epsilon distribution” (RED). For discontinuous structures, the reconstructed distribution shows typical Gibbs phenomena, i.e. oscillations at the edges. Although the period and the spatial extent of these oscillations decreases with the mode number M , the amplitude remains practically constant also for very large mode numbers.

3.2 TM-polarisation

The situation for TM polarisation is slightly more complicated for than for TE-polarisation. The magnitude square of the electric field $|\mathbf{E}|^2 = |E_x|^2 + |E_z|^2$ now also requires the z-component of the electric field. With TM-polarisation, the x-component of the electric field is similarly expressed by:

$$E_x(x, z) = \sum_m S_m(z) \exp(ik_{x,m}x) \quad (17)$$

with $k_{x,m}$ identical to the definition in Eq. (14). Note that $\mathbf{S}(z) = -i \mathbf{V} \cdot \mathbf{D}(z)$ differs from the TE-case and the D -vector is $D_m(z) = -c_m^+ \exp(-k_0 z \sqrt{\lambda_m}) + c_m^- \exp(k_0(z-d) \sqrt{\lambda_m})$. According to ref [2], $\mathbf{S}(z)$ in this case is derived from the vector $\mathbf{V} = \mathbf{E}_a \mathbf{W} \mathbf{Q}$, which contains the Töplitz matrix \mathbf{E}_a of the inverse of the permittivity distribution, the eigenvector matrix \mathbf{W} and the eigenvalue matrix $\mathbf{Q} = \text{diag}(\sqrt{\Lambda})$. With this, the z-component of the electric field is derived from the derivative of the H-field as:

$$E_z(x, z) = -\sum_m u_m(z) \exp(ik_{x,m}x) \quad (18)$$

with $\mathbf{u} = \mathbf{E}^{-1} \left(\frac{\mathbf{K} \mathbf{X}}{k_0} \mathbf{U} \right)$ and $\mathbf{U} = \mathbf{W} \cdot \mathbf{C}(z)$ as the coefficient vector for the H-field. This choice

for the z-component is consistent with the inverse rule [6]. In the comparisons which follow, we will label this choice definitions for the x- and z-components of the electric field, as (TM1). The definition of E_x in Eq. (17) leads to a field, which is continuous in z-direction and in x-direction. The continuity in z-direction follows from Maxwell's equations since E_x is

a tangential component. The continuity in x -direction follows from the mode limitation and is not physical for discontinuous structures. Therefore Lalanne [5] has proposed an alternative definition for the calculation of the TM near-field. In his definition, E_x is derived from the D-field by

$$E_x(x, z) = \frac{1}{\varepsilon(x)} \sum_m d_m(z) \exp(ik_{x,m}x) \quad (19)$$

with the vector $\mathbf{d}(z) = -i \mathbf{W} \cdot \mathbf{Q} \cdot \mathbf{D}(z)$. Since the inverse rule is not applied, E_x becomes discontinuous in x -direction. E_x also becomes discontinuous in z -direction, which is in disagreement with the assumption that E_x is a tangential component. We therefore modify the definition of Lalanne slightly in the sense that

$$E_x(x, z) = \sum_m e_m(z) \exp(ik_{x,m}x) \quad (20)$$

with $\mathbf{e}(z) = -i \mathbf{E}^{-1}(\mathbf{W} \cdot \mathbf{Q} \cdot \mathbf{D}(z))$. With this definition, E_x is compatible with the inverse rule. In the following we will refer to this choice as (TM2). For the calculation of local absorption using the formula of Eq. (11), we now have a combination of $\varepsilon(x, z)$ calculated by (OED, RED) and $E_x(x, z)$ calculated by (TM1, TM2). For the z -component, no deviation from Eq. (18) is necessary.

4. Numerical results

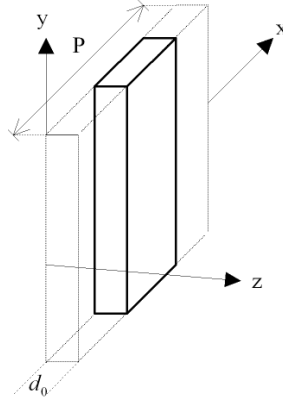


Fig. 1. Grating geometry

For the numerical analysis, we have considered the following test case. We assume that the incident region has an index of refraction of $n_i = 3.65$, the transmitted region is air with $n_t = 1$ and the layer region contains a symmetric grating with a period $P = 0.6 \mu\text{m}$, a thickness of $d = 0.3 \mu\text{m}$ and two regions of equal diameter with $\varepsilon_1 = 13.3 + 0.025i$ and $\varepsilon_2 = 1 + 0i$. The incident wave has a wavelength of $1 \mu\text{m}$ and enters at perpendicular incidence, propagating in the positive z -direction. For the RCWA-calculation, we use 4 modes, i.e. $M = 4$ in all examples. Figure 1 shows the grating geometry. The grating period P extends in x -direction. The grating is constant in y -direction. The grating consists of layers $0 \leq l < L$ each with a thickness d_l starting at $z = 0$ and extending in the positive z -direction. In the successive Figs. 2, 3, 4 and 6, the horizontal axis is the z -axis in microns, the vertical axis is the x -axis, also in microns.

4.1 Field calculation for the TE case

For the TE-case, the RCWA-calculation results in a global absorption of $A_g = 3.540\%$. The local absorption is shown in Fig. 2 together with the values for the integrated absorption. The left part of Fig. 2 shows the OED-case and the right part the RED-case. Due to mode limitation, the edges are soft for the RED-case.

We see, that for TE-polarization, the choice of exact (OED) or mode-limited ε (RED) makes no significant difference and the integrated absorption agrees sufficiently well with the global absorption. The difference amounts to 0.6% for only 4 modes.

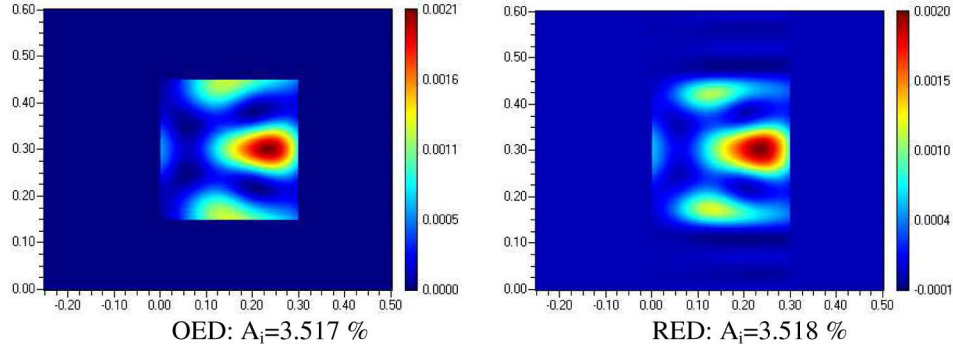


Fig. 2. Local absorption for the TE-case. Left with true spatial ε -distribution, right with reconstructed ε -distribution.

4.2 Field calculation for the TM case

For the TM-case, we numerically obtain a global absorption of $A_g = 1.389\%$ from the RCWA. Again, the local absorption is shown in Fig. 3 together with the values for the integrated absorption.

One can observe again, that the choice of exact versus reconstructed ε -distribution does not show a significant influence on the integrated absorption. In Fig. 4 the results for the modified field definition according to Eq. (20) are shown. It is clear that the modified definition for the electric field provides integrated absorption values, which agree significantly better with the global absorption (0.6% deviation) than the traditional definition (5% deviation).

Figure 5 illustrates this behaviour depending on the number of modes used in the calculation. It shows, that the modified definition for any number of modes is preferable to the standard definition.

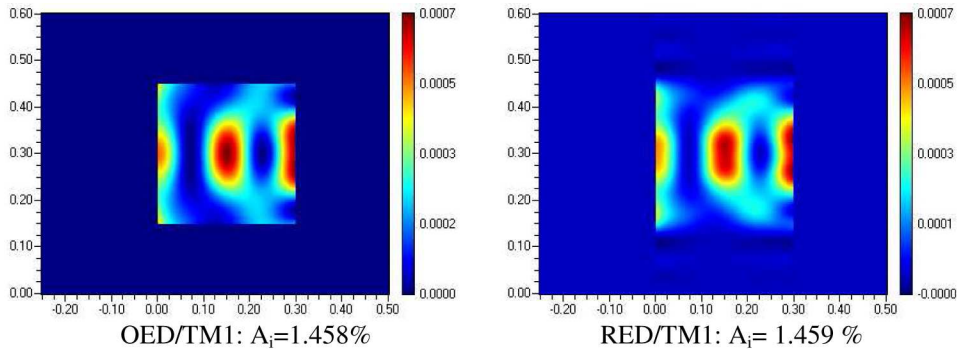


Fig. 3. Local absorption for the TM-case. Left with exact spatial ε -distribution, right with reconstructed ε -distribution, using the standard field definitions.

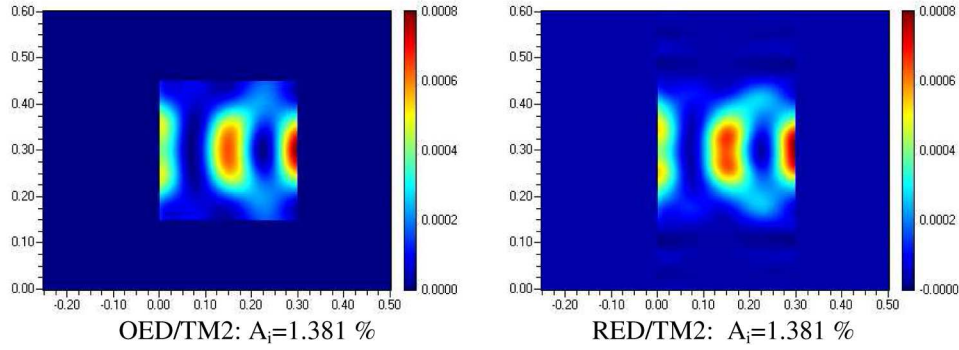


Fig. 4. Local absorption for the TM-case. Left with exact spatial \mathcal{E} -distribution, right with reconstructed \mathcal{E} -distribution, using the modified field definitions from Eq. (20). The results agree much better with the global absorption value of 1.389%.

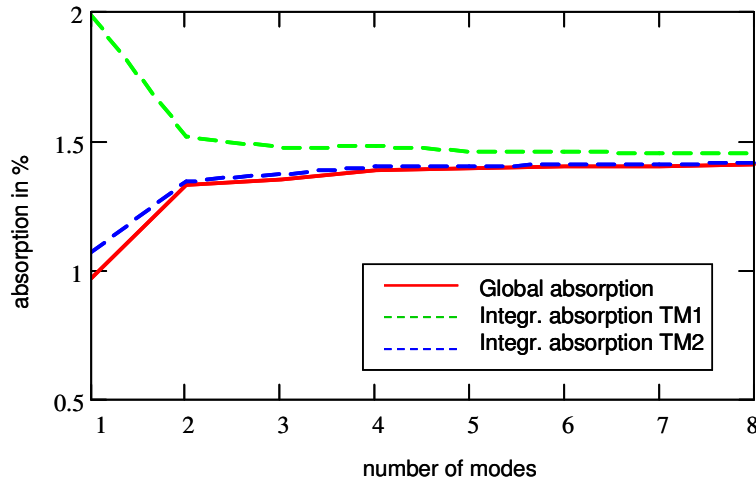


Fig. 5. Comparison of global and integrated absorption for different number of modes. The blue curve was calculated with the modified field definition while the green curve was calculated with the standard field definition.

5. Example

In the following, we have selected a more complex example: a stacked grating with six layers. The grating period is $0.4 \mu\text{m}$ and two periods are shown in Fig. 6. The layers consist of semiconductor and polymer sections. The calculations are performed with 6 modes. By illuminating this structure with different wavelength in the range from 400 to 700 nm, the global absorption does not vary significantly, but we can see in Fig. 6 that the local absorption in the first grating is affected significantly by a change in wavelength. The left part of Fig. 6 shows the local absorption at 425 nm wavelength. The global absorption in this case is 82.13% the integrated absorption with the modified definition is 83.18% and the integrated absorption with the standard definition is 86%. The right part of Fig. 6 shows the local absorption at 675 nm wavelength. The global absorption in this case is 58.6% the integrated absorption with the modified definition is 58.8% and the integrated absorption with the standard definition is 60%. For a detector design, for example, such a change in local absorption can be very relevant, if the depletion region would be near the first grating (layer 1 and 2). In the 675 nm case, most of the light is absorbed in the second grating (layer 4 and 5), which would not contribute to photocurrent.

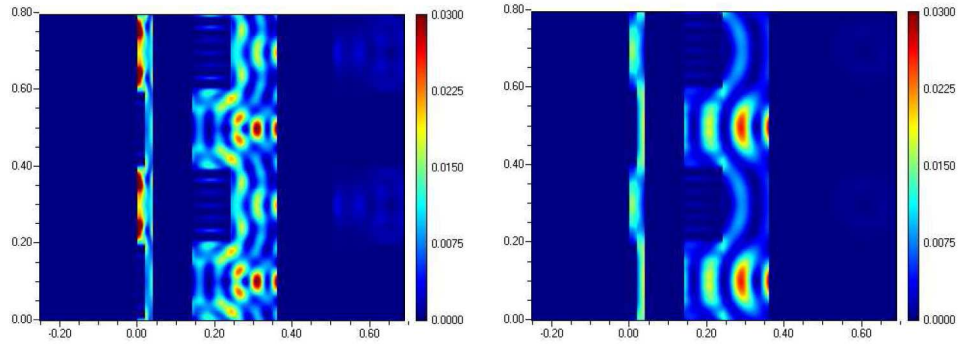


Fig. 6. Local absorption in a stacked grating structure for different wavelength. Left: exposure at 425 nm, Right: exposure at 675 nm wavelength.

6. Summary

We have derived an equation for determining the local amount of power dissipated in a given volume. The result can be applied directly to field calculations from standard rigorous methods assuming an incident field amplitude of unity. Furthermore, we have observed, that for the calculation of electric near field components in the TM-case, the definition in Eq. (20) leads to results, which converge better, i.e. the results for a small number of modes is more similar to the fields obtained by taking a very large number of modes. Furthermore, the modified definition also leads to a better agreement between the global absorption obtained from the law of energy conservation and the integrated absorption obtained by integration over the local absorption.